RSC Advances

PAPER

View Article Online
View Journal | View Issue

Cite this: *RSC Adv.*, 2017, **7**, 845

Cm-size free-standing self-organized buckypaper of bucky-onions filled with ferromagnetic Fe_3C†

Filippo S. Boi,*[a] Jian Guo,[a] Gang Xiang,[a] Mu Lan,[a] Shanling Wang,[b] Jiqiu Wen,[b] Sijie Zhang[a] and Yi He[b]

Received 10th October 2016
Accepted 9th November 2016

DOI: 10.1039/c6ra24983c

www.rsc.org/advances

Novel cm-size free-standing buckypapers of bucky-onions filled with a single-phase of ferromagnetic Fe_3C single crystals were serendipitously discovered. These buckypapers are obtained directly *in situ* as the dominant product of the pyrolysis of ferrocene. Vibrating sample magnetometry also revealed an extremely large coercivity of 0.120 tesla and a saturation magnetization of 41 emu g^{-1}.

Introduction

Since 1985, novel carbon nanostructures such as Buckminster fullerene (C_{60}),[1,2] carbon nanotubes (CNTs),[3,4] bucky-onions[5,6] and recently graphene[7] have attracted the attention of numerous research groups owing to their exceptional physical and chemical properties. In particular, the high chemical stability of C_{60},[1,2] bucky-onions[5,6] and CNTs[3,4,8–14] make these structures ideal nanocapsules that can be filled with a specific material of interest.[8–17] However, despite the numerous reports in the literature, the nucleation mechanism of these nanostructures is not well understood and remains strongly controversial.[18–21]

In 1997 Elliot *et al.*[19] suggested that two main parameters are responsible for the nucleation and growth of carbon nanostructures: the local-path carbon-to-metal ratio (LCM) and the global carbon-to-metal ratio (GCM). LCM refers to metal particles having the same local conditions along the same spatial pathway, while the GCM determines the weighting between different LCMs and is generally defined by the stoichiometry of the molecule used as precursor. Chemical vapour deposition (CVD) techniques have been generally designed to avoid local pathway fluctuations.[8–17]

Interestingly the research works reported by Raty *et al.*[20] and Anna Moisala *et al.*[21] proposed two mechanism of nanotube nucleation from heterogeneously nucleated particles. The first mechanism[20] involves the formation of a floating graphene-cap and can be divided into three step: (i) diffusion of single carbon atoms on the surface of the catalyst, (ii) formation of a graphene sheet floating on the catalyst surface with edge atoms covalently bonded to the metal, (iii) root incorporation of diffusing single C atoms.

Differently, a nucleation process involving the formation of islands of C atoms was proposed by Moisala *et al.*[21] (second mechanism). In this process, the competition between two fluxes of carbon was described. These fluxes were identified as (1) the segregation flux of dissolved carbon atoms towards the particle surface and (2) the diffusion flux of carbon atoms toward the particle surface seeking their lowest energy states. Due to the competition between the segregation and diffusion fluxes, two situations would then occur in the system. (i) First situation: if the segregation flux is higher than the diffusion flux, initiation of CNT growth can occur; (ii) second situation: if the segregation flux is lower than the diffusion flux, carbon will form the thermodynamically most stable system consisting of metal particles surrounded by graphitic layers (bucky-onions).

These synthesis products have attracted the attention of numerous researchers for applications in magnetic data storage system, exchange bias systems,[8–17] supercapacitors and power-storage systems[22–27] (owing to their resistance–inductance–capacitance properties). However, despite the nucleation and growth models described above, the control of these processes through CVD approaches remains challenging and depends strongly on the CVD parameters (*i.e.* reactor design, vapour flow-rate, pyrolyzed vapour concentration). Numerous approaches have been developed for the creation of magnetic and non-magnetic films[10,22–25] and gels[26] suitable for the applications listed above. However, the *in situ* synthesis of large scale buckypapers comprising bucky-onions remains challenging. Interestingly recent works from Boi *et al.*[28] have shown that CNTs urchin-structures with a core composed of Fe_3C, γ-Fe and α-Fe filled bucky-onions can be obtained in conditions of locally perturbed vapour-flow, in the viscous boundary layer created at the boundary between a rough substrate-surface and the main Ar gas-flow.[28]

In this paper we report another effect of the locally perturbed vapour flow induced by the flow-facing leading edge of the used substrate. We find that cm-size free-standing buckypapers of bucky-onions filled with a single-phase of ferromagnetic Fe_3C single crystals (Fe_3C-filled CPBO) can be grown on the leading

[a]College of Physical Science and Technology, Sichuan University, Chengdu, China. E-mail: f.boi@scu.edu.cn

[b]Analytical and Testing Centre, Sichuan University, Chengdu, China

† Electronic supplementary information (ESI) available. See DOI: 10.1039/c6ra24983c

edge of a silicon-substrate and on the top of CNTs films and directly removed with a permanent magnet. These structures are obtained directly *in situ* in cm scale through the pyrolysis of ferrocene with very low flow-rates. Differently, if no silicon substrate is used, CNTs-films were obtained in the inner wall of the reactor. The morphology of these structures is investigated through scanning electron microscopy (SEM). The cross-section, single crystal arrangement and phase-composition of the encapsulated crystals is demonstrated through transmission electron microscopy (TEM) and high resolution TEM (HRTEM). The single-phase Fe_3C filling is demonstrated through X-ray diffraction (XRD) analyses while the magnetic properties are investigated through vibrating sample magnetometry (VSM). An extremely large coercivity of 0.120 tesla and a saturation magnetization of 41 emu g^{-1} were measured.

Experimental

Cm-size Fe_3C-filled CPBO were obtained by sublimation and pyrolysis of 180–200 mg of ferrocene in an Ar flow of 11 ml $minute^{-1}$ on the top of Si/SiO_2 substrates positioned inside a quartz tube reactor of length 1.5 metres. A one-zone electrical furnace was used for reaching the desired temperature of pyrolysis (temperature of 990 °C). The sublimation temperature was 500 °C. The used reaction time was 25 min. A fast cooling method was used to bring the Fe_3C-filled CPBO to room temperature. In this method, cooling times of approximately 20 min were achieved by removing the furnace along a rail system (quench).

The Fe_3C-filled CPBO was removed through the use of a permanent magnet from the upper-surface of aligned CNTs grown on the Si/SiO_2 substrates and from the first edge of the Si/SiO_2 substrates (edge facing the Ar flow). SEM investigations of the morphology of the obtained Fe_3C-filled CPBO were performed with a JSM-7500F at 15 kV. TEM and HRTEM investigations were performed using a 200 kV American FEI Tecnai G^2F20 fitted with field emission gun. XRD analyses were performed with a Philips Xpert pro MPD (Cu Kα with $\lambda = 0.154$ nm). In order to identify the phases composing the Fe_3C-filled CPBO and extract the unit cell values, the Rietveld refinement method was used. The magnetic measurements were performed at room temperature by employing a VSM 2.5 tesla electromagnet East Changing 9060 at the magnetic field of 1.3 tesla.

Results and discussion

SEM micrographs revealed the morphology of the Fe_3C-filled CPBO. A typical example of the morphology is shown in Fig. 1A with a top view and in Fig. 1B with a closer view.

Note that the morphology of the Fe_3C-filled CPBO was slightly damaged due to the pressing procedure necessary for the SEM sample preparation. The crystal-structure and crystal symmetry of the Fe_3C-filled CPBO was investigated through XRD analyses. A typical XRD diffractogram of the Fe_3C-filled CPBO is shown in Fig. 2A.

The CPBO structure was identified by the 002 peak of graphitic carbon with space group $P6_3/mmc$. The Fe_3C filling was

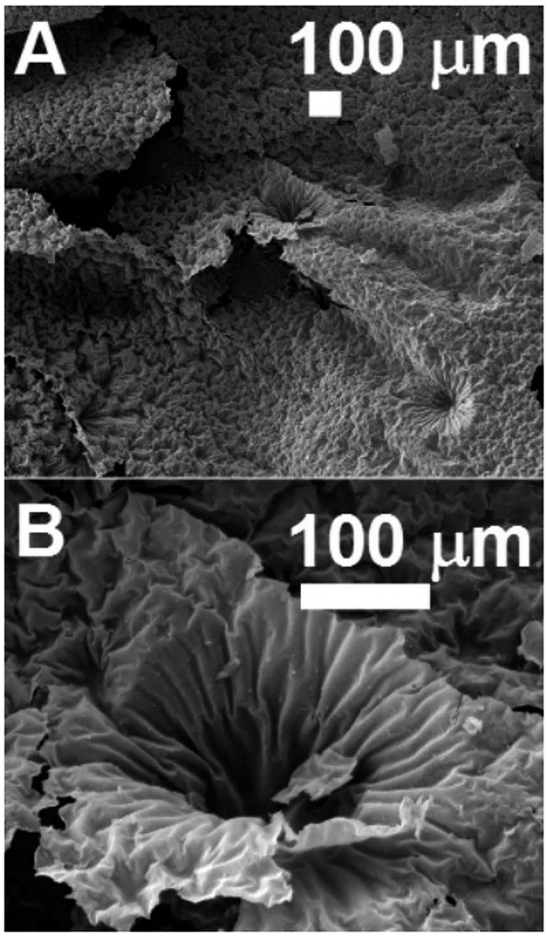

Fig. 1 Scanning electron micrographs (A and B) showing the morphology of a typical cm size free standing Fe_3C-filled CPBO. See ESI† for SEM images with higher detail and example of energy dispersive X-rays analyses.

instead identified by the 111, 200, 210, 002, 201, 211, 102, 220, 031, 112, 131, 221 and 122 reflections. Two reflections of Fe_2O_3 were also observed (104 and 110 reflections). These observations suggest that each bucky-onion composing the CPBO is filled with a single phase of Fe_3C. Instead the small Fe_2O_3 reflections can be associated to particles not completely covered with graphitic layers that oxidize after sample extraction, due to interaction with oxygen.

This interpretation is confirmed by the Rietveld refinement shown in Fig. 2B. The relative abundances of 95% of Fe_3C and 5% of Fe_2O_3 were extracted (in order to compare the relative abundance of Fe_3C and Fe_2O_3 the graphitic carbon contribution was excluded from the refinement). The extracted unit-cell parameters from the Rietveld refinement are as follow:

(1) Fe_3C $a = 0.51$ nm, $b = 0.68$ nm, $c = 0.45$ nm orthorhombic with space group *Pnma*,

(2) Fe_2O_3 $a = 0.51$ nm $b = 0.51$ nm $c = 1.38$ nm rhombohedral with space group $R\bar{3}ch$.

The cross section and the single-crystal arrangement of the Fe_3C-filled CPBO phase were then investigated through TEM and HRTEM. The homogeneity of the CPBO was revealed by the TEM micrographs of Fig. 3A and B.

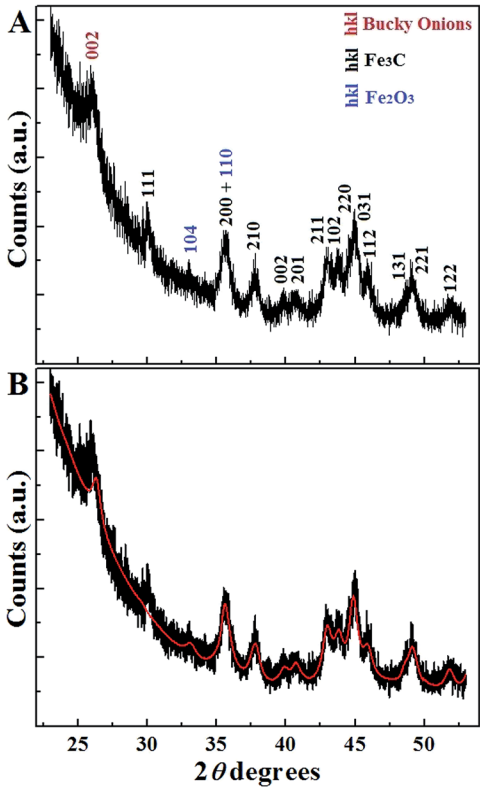

Fig. 2 X-ray diffractogram (A) and Rietveld refinement (B) of a typical cm size free standing Fe_3C-filled CPBO. Each peak is labelled with the corresponding crystal-plane reflection.

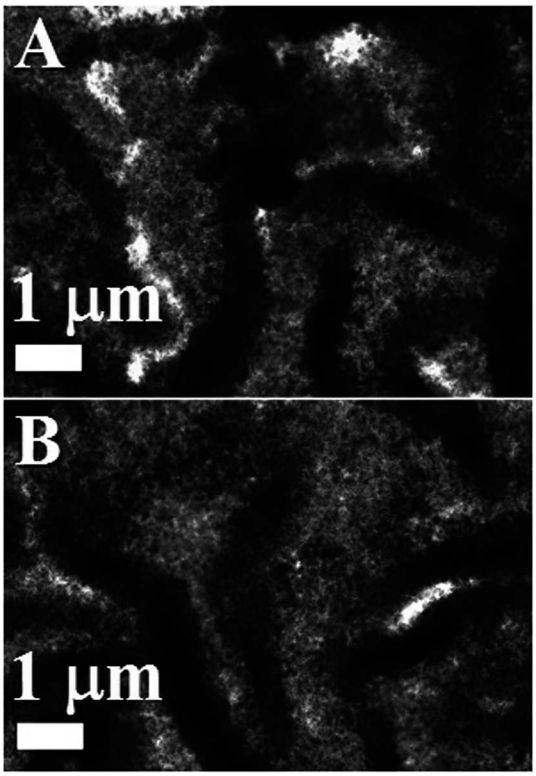

Fig. 3 TEM micrographs showing in A and B the cross-section of a typical Fe_3C-filled CPBO.

Note that the black regions represent thick-areas in which the CPBO structure appears to be bent.

A higher detail of the cross section of the Fe_3C-filled CPBO structure is shown in Fig. 4 where large quantities of Fe_3C-filled bucky-onions can be clearly observed.

The bucky-onions composing the CPBO appear to interact between each other with van der Waals forces. We will show later that the origin of such close contact in the long range has to be associated to the nucleation mechanism of these structures. Such close-contact between the onions-structures was also confirmed by the HRTEM analyses (see Fig. 5A and B) where a high detail of the connection between two bucky-onions is shown. Note that the lattice fringes observed in the onion structure in Fig. 5A correspond to the graphitic interatomic distance between the 002 planes. The observation of this interatomic distance is in agreement with the XRD analyses in Fig. 2. The single-crystal arrangement of the encapsulated Fe_3C phase was confirmed by the observation of a preferred lattice orientation in the HRTEM analyses of the crystals encapsulated in single bucky-onions. This interpretation is also confirmed by the FFT of the area shown in Fig. 5B were a single pattern of reciprocal lattice spots is found. The yellow circles indicate the 211 reflections of orthorhombic Fe_3C with space group *Pnma* corresponding to a lattice spacing of 0.211 nm. The red circles indicate the 101 reflection of orthorhombic Fe_3C with space group *Pnma* corresponding to a lattice spacing of 0.338 nm.

The presence of a single phase of Fe_3C within the CPBO can be considered a consequence of the fast cooling rate imposed by the furnace removal. Also, the presence of numerous graphitic layers surrounding the Fe_3C particles suggest that the CPBO is formed directly in the pyrolyzed ferrocene-vapour during the

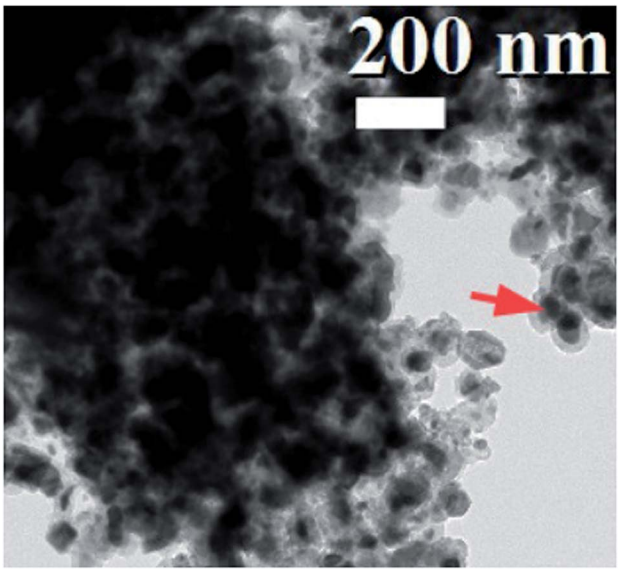

Fig. 4 TEM micrograph showing with higher detail the Fe_3C-filled bucky-onions comprised in the CPBO. A typical example of a Fe_3C particle is indicated with the red arrow.

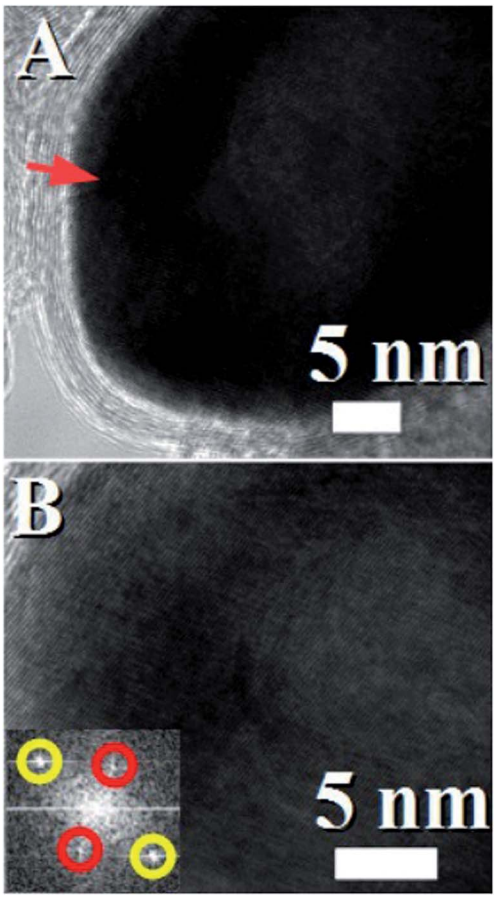

Fig. 5 HRTEM micrographs (A and B) showing with high detail the cross section of a typical bucky-onion (comprised in the CPBO structure) filled with a Fe_3C single crystal (indicated by the red arrow). In B the FFT of the crystal lattice shows (in the inset) a single set of reciprocal lattice spots which proves the single crystal arrangement of Fe_3C.

reaction time of 25 min and not during the cooling process. These observations suggest therefore a mechanism of formation different with respect to what described in previous reports by Elliot *et al.* and Moisala *et al.*[19,21] where the formation of bucky-onions is considered favourable only with slow cooling rates and slow carbon supply or in conditions where the diffusion carbon flux is dominant.

Indeed it was shown that the mechanism of formation of bucky-onions in W-arc processes depends mainly on the kinetics of carbon supply. Similarly to Moisala *et al.*,[21] two types of carbon supply were identified: expulsion (from the particle core to the external surface) and deposition (from the external surface to the particle core). For slow growth processes the final product was found to depend on the difference between the particle-graphite interface energy and the vacuum surface energies γ, and the energy to bend the graphite sheets.[19] The formation of bucky-onions was then associated to growth-conditions with low γ interaction.[19] However considering our CVD system, the vacuum surface energies can not be considered since an Ar carrier-gas is used to deliver the ferrocene-vapour and clean the system from oxygen impurities. We suggest that the mechanism of formation of the Fe_3C-filled CPBO depends strongly on the boundary-layer mechanism; note that the boundary layer is created between the substrate-edge (facing the Ar flow) and the Ar flow as shown in Fig. 6A. The bucky-onions can be considered a consequence of a spontaneous homogeneous nucleation process of Fe-based particles induced by the local boundary layer created at the edge of the Si/SiO_2 substrate. The CPBO was indeed observed in the edge of the Si/SiO_2 substrate and on the top of aligned multiwall CNTs grown on the substrate surface from heterogeneously nucleated particles. A schematic of the substrate before and after the CPBO growth is shown in Fig. 6A and B. The formation of such ordered buckypaper can be therefore attributed to the very high concentration of homogeneously nucleated particles produced in the boundary layer vapour and their physical interactions after nucleation and encapsulation. The magnetic properties of the Fe_3C-filled CPBO were then investigated by VSM. A typical hysteresis loop is shown in Fig. 7. Interestingly a very large coercivity of 0.120 tesla and a saturation magnetization of 41 emu g^{-1} were measured. The measured saturation magnetization is much lower with respect to what expected for a bulk sample of Fe_3C ($M_s = 169$ emu g^{-1}, $T = 483$ K).[29] This difference could be attributed to the nano-crystalline nature of the sample. However, the observed coercivity is much larger with respect to what expected for nanocrystalline Fe (23 Oe) and for polycrystalline Fe (1 Oe).[29] These observations suggest that a fundamental role can be attributed to the strong magnetocrystalline anisotropy (spin–orbit) contribution in the Fe_3C crystals that controls the coercivity of the Fe_3C nanoparticles. The

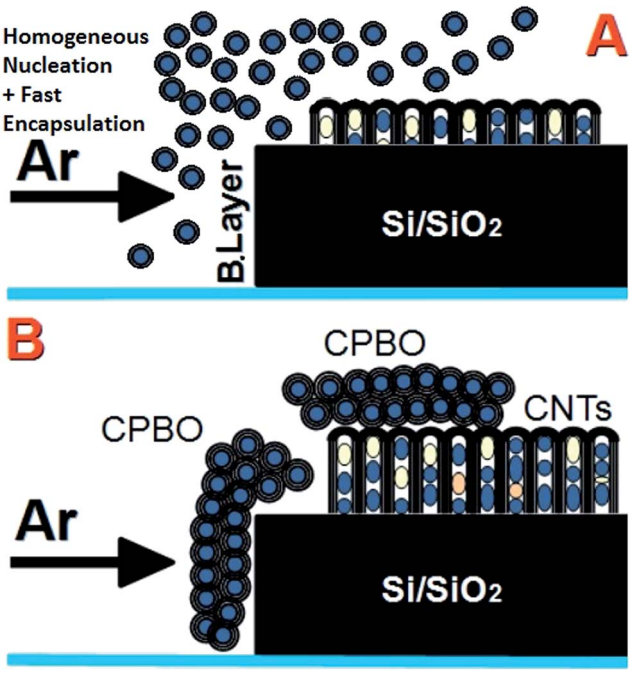

Fig. 6 Schematic of the boundary layer and the deposition area (A and B) of the CPBO inside the quartz tube reactor. The quartz tube reactor is indicated with cyan colour, the Si/SiO_2 substrate is indicated with black colour. The Fe_3C crystals are indicated with blue colour, the γ-Fe and the α-Fe phases are indicated with yellow and light orange colours respectively.

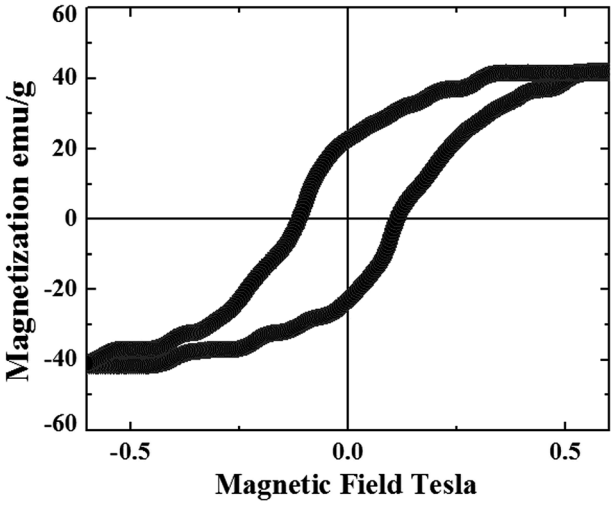

Fig. 7 Hysteresis loop measured from 3 CPBO of cm-size comprising bucky-onions filled with Fe_3C single crystals with an average diameter of 30 nm.

observed coercivity is indeed much larger with respect to that measured at room temperature in the case of the ferromagnetic bucky-paper produced by Ruitao Lv *et al.* (500 Oe at 300 K)[10] suggesting therefore that the magnetocrystalline anisotropy has a fundamental role in the magnetic properties of the CPBO. Instead the saturation magnetization is comparable with that measured by Ruitao Lv *et al.*[10] The observation of small Fe_2O_3 reflections suggests that a very small fraction of nanoparticles are not covered completely with graphitic layers. These particles may be formed in the last stages of the CPBO growth when the carbon concentration in the pyrolyzed ferrocene vapour is lower. Therefore, considering the presence of 5% of Fe_2O_3 in the sample (observed with XRD), a magnetic contribution to the saturation magnetization (*i.e.* exchange coupling) from this phase can not be excluded.

Conclusion

In conclusion we reported the serendipitous discovery of novel cm-size free-standing papers of bucky onions filled with a single-phase of ferromagnetic Fe_3C single crystals. These structures are obtained directly *in situ* from the pyrolysis of ferrocene on the leading edge of a Si/SiO_2 substrate and on the top of aligned partially filled CNTs. An extremely large coercivity of 0.120 tesla and a saturation magnetization of 41 emu g^{-1} were measured at room temperature. The magnetic properties and the large scale of these buckypapers can open new avenues toward the development of magnetic data storage, magnetic refrigeration systems and thermoelectrics. In addition these materials could be considered for applications in catalysis,[30] supercapacitors,[30] energy-storage,[31] miniaturised fuel cells,[32] biomedicine[33] and many others.

Acknowledgements

We acknowledge Prof. Gong Min for his continuous support in this research work. We are also grateful for the NSFC 11404227.

References

1 H. W. Kroto, J. R. Heath, S. C. O'Brien, R. F. Curl and R. E. Smalley, C_{60}: Buckminsterfullerene, *Nature*, 1985, **318**, 162–163.
2 L. Hultman, S. Stafstrom, Z. Czigany, J. Neidhardt, N. Hellgren, I. F. Brunell, K. Suenaga and C. Colliex, Cross-Linked Nano-onions of Carbon Nitride in the Solid Phase: Existence of a Novel $C_{48}N_{12}$ Aza-Fullerene, *Phys. Rev. Lett.*, 2001, **87**, 225503.
3 S. Iijima, Helical microtubules of graphite carbon, *Nature*, 1991, **354**, 56–58.
4 S. Iijima and T. Ichihashi, Single-shell carbon nanotubes of 1 nm diameter, *Nature*, 1993, **363**, 603–605.
5 D. Ugarte, Curling and closure of graphitic networks under electron-beam irradiation, *Nature*, 1992, **359**, 707–709.
6 N. Sano, H. Wang, M. Chhowalla, I. Alexandrou and G. A. J. Amaratunga, Nanotechnology: Synthesis of carbon'onions' in water, *Nature*, 2001, **414**, 506–507.
7 K. S. Novoselov, A. K. Geim, S. V. Morozov, D. Jiang, Y. Zhang, S. V. Dubonos, I. V. Grigorieva and A. A. Firsov, Electric Field Effect in Atomically Thin Carbon Films, *Science*, 2004, **306**, 666–669.
8 R. S. Ruoff, D. C. Lorents, B. Chan, R. Malhotra and S. Subramoney, Single Crystal Metals Encapsulated in Carbon Nanoparticles, *Science*, 1993, **259**, 346–348.
9 H. Terrones, F. Lopez-Urias, E. Munoz-Sandoval, J. A. Rodriguez-Manzo, A. Zamudio, A. L. Elias and M. Terrones, Magnetism in Fe-based and carbon nanostructures: theory and applications, *Solid State Sci.*, 2006, **8**, 303–320.
10 R. Lv, S. Tsuge, X. Gui, K. Takai, F. Kang, T. Enoki, J. Wei, J. Gu, K. Wang and D. Wu, *In situ* synthesis and magnetic anisotropy of ferromagnetic buckypaper, *Carbon*, 2009, **47**, 1141–1145.
11 F. C. Dillon, A. Bajpai, A. Koos, S. Downes, Z. Aslam and N. Grobert, Tuning the magnetic properties of iron-filled carbon nanotubes, *Carbon*, 2012, **50**, 3674–3681.
12 A. Morelos-Gomez, F. Lopez-Urias, E. Munoz-Sandoval, C. L. Dennis, R. D. Shull, H. Terrones and M. Terrones, Controlling high coercivities of ferromagnetic nanowires encapsulated in carbon nanotubes, *J. Mater. Chem.*, 2010, **20**, 5906–5914.
13 S. Hampel, A. Leonhardt, D. Selbmann, K. Biedermann, D. Elefant, C. h. Muller, T. Gemming and B. Buchner, Growth and characterization of filled carbon nanotubes with ferromagnetic properties, *Carbon*, 2006, **44**, 2316–2322.
14 U. Weissker, M. Loffler, F. Wolny, M. U. Lutz, N. Scheerbaum, R. Klingeler, T. Gemming, T. Muhl, A. Leonhardt and B. Buchner, Perpendicular magnetization of long iron carbide nanowires inside carbon nanotubes due to magnetocrystalline anisotropy, *J. Appl. Phys.*, 2009, **106**, 054909.
15 M. U. Lutz, U. Weissker, F. Wolny, C. Muller, M. Loffler, T. Muhl, A. Leonhardt, B. Buchner and R. Klingeler, Magnetic properties of a-Fe and Fe_3C nanowires, *J. Phys.: Conf. Ser.*, 2010, **200**, 072062.

16 A. Leonhardt, M. Ritschel, D. Elefant, N. Mattern, K. Biedermann, S. Hampel, C. h. Muller, T. Gemming and B. Buchner, Enhanced magnetism in Fe-filled carbon nanotubes produced by pyrolysis of ferrocene, *J. Appl. Phys.*, 2005, **98**, 074315.

17 A. Leonhardt, M. Ritschel, R. Kozhuharova, A. Graffa, T. Muhl, R. Huhleb, I. Monch, D. Elefant and C. M. Schneider, Synthesis and properties of filled carbon nanotubes, *Diamond Relat. Mater.*, 2003, **12**, 790–793.

18 A. K. Schaper, H. Hou, A. Greiner and F. Phillipp, The role of iron carbide in multiwalled carbon nanotube growth, *J. Catal.*, 2004, **222**, 250–254.

19 B. R. Elliott, J. J. Host, V. P. Dravid, M. H. Teng and J. H. Hwang, A descriptive model linking possible formation mechanisms for graphite-encapsulated nanocrystals to processing parameters, *J. Mater. Res.*, 1997, **12**, 3328–3344.

20 J. Y. Raty, F. Gygi and G. Galli, Growth of Carbon Nanotubes on Metal Nanoparticles: A Microscopic Mechanism from Ab Initio Molecular Dynamics Simulations, *Phys. Rev. Lett.*, 2005, **95**, 096103.

21 A. Moisala, A. G. Nasibulin and E. I. Kauppinen, The role of metal nanoparticles in the catalytic production of single-walled carbon nanotubes a review, *J. Phys.: Condens. Matter*, 2003, **15**, S3011–S3035.

22 M. Endo, H. Muramatsu, T. Hayashi, Y. A. Kim, M. Terrones and N. S. Dresselhaus, Nanotechnology: 'buckypaper' from coaxial nanotubes, *Nature*, 2005, **433**, 476.

23 W. Ding, S. Pengcheng, L. Changhong, W. Wei and F. Shoushan, Highly oriented carbon nanotube papers made of aligned carbon nanotubes, *Nanotechnology*, 2008, **7**, 075609.

24 P. D. Bradford, X. Wang, H. Zhao, J. P. Maria, Q. Jia and Y. T. Zhu, A novel approach to fabricate high volume fraction nanocomposites with long aligned carbon nanotubes, *Compos. Sci. Technol.*, 2010, **70**, 1980–1985.

25 M. T. Byrne and Y. K. Gunko, Recent Advances in Research on Carbon Nanotube-Polymer Composites, *Adv. Mater.*, 2010, **22**, 1672–1688.

26 M. B. Bryning, D. E. Milkie, M. F. Islam, L. A. Hough, J. M. Kikkawa and A. G. Yodh, Carbon Nanotube Aerogels, *Adv. Mater.*, 2007, **19**, 661–664.

27 C. M. Schnitzler, M. M. Oliveira, D. Ugarte and A. J. G. Zarbin, One-step route to iron oxide-filled carbon nanotubes and bucky-onions based on the pyrolysis of organometallic precursors, *Chem. Phys. Lett.*, 2003, **381**, 541–548.

28 F. S. Boi, G. Mountjoy and M. Baxendale, Boundary layer chemical vapor synthesis of self organized radial filled-carbon-nanotube structures, *Carbon*, 2013, **64**, 516–526.

29 S. Karmakar, S. M. Sharma, M. D. Mukadam, S. M. Yusuf and A. K. Sood, Magnetic behaviour of iron-filled multiwalled carbon nanotubes, *J. Appl. Phys.*, 2005, **97**, 054306.

30 R. Borgohain, J. Yang, J. P. Selegue and D. Y. Kim, Controlled synthesis, efficient purification and electrochemical characterization of arc-discharge carbon nano-onions, *Carbon*, 2014, **66**, 272–284.

31 D. Pech, M. Brunet, H. Dorou, P. H. Huang, V. Mochalin, Y. Gogotsi, *et al.*, Ultrahigh power micrometre-sized supercapacitors based on onion-like carbon, *Nat. Nanotechnol.*, 2010, **5**, 651–654.

32 A. S. Rettenbacher, B. Elliott, J. S. Hudson, A. Amirkhanian and L. Echegoyen, Preparation and functionalization of multilayer fullerenes (carbon nano-onions), *Chem.–Eur. J.*, 2006, **12**, 376–387.

33 A. Palkar, A. Kumbhar, A. J. Athans and L. Echegoyen, Pyridyl-functionalized and water soluble carbon nano onions: first supramolecular complexes of carbon nano onions, *Chem. Mater.*, 2008, **20**, 1685–1687.